Eur Biophys J (2015) 44:383–391
DOI 10.1007/s00249-015-1043-8

ORIGINAL PAPER

EBSA
Biophysics in Europe

Elucidating how bamboo salt interacts with supported lipid membranes: influence of alkalinity on membrane fluidity

Jong Hee Jeong[6] · Jae-Hyeok Choi[1,2] · Min Chul Kim[1,2] · Jae Hyeon Park[1,2] · Jason Scott Herrin[1] · Seung Hyun Kim[5] · Haiwon Lee[4,6] · Nam-Joon Cho[1,2,3]

Received: 11 December 2014 / Revised: 2 May 2015 / Accepted: 13 May 2015 / Published online: 24 May 2015

Abstract Bamboo salt is a traditional medicine produced from sea salt. It is widely used in Oriental medicine and is an alkalizing agent with reported antiinflammatory, antimicrobial and chemotherapeutic properties. Notwithstanding, linking specific molecular mechanisms with these properties has been challenging to establish in biological systems. In part, this issue may be related to bamboo salt eliciting nonspecific effects on components found within these systems. Herein, we investigated the effects of bamboo salt solution on supported lipid bilayers as a model system to characterize the interaction between lipid membranes and bamboo salt. The atomic composition of unprocessed and processed bamboo salts was first analyzed by mass spectrometry, and we identified several elements that have not been previously reported in other bamboo salt preparations. The alkalinity of hydrated samples was also measured and determined to be between pH 10 and 11 for bamboo salts. The effect of processed bamboo salt solutions on the fluidic properties of a supported lipid bilayer on glass was next investigated by fluorescence recovery after photobleaching (FRAP) analysis. It was demonstrated that, with increasing ionic strength of the bamboo salt solution, the fluidity of a lipid bilayer increased. On the contrary, increasing the ionic strength of near-neutral buffer solutions with sodium chloride salt diminished fluidity. To reconcile these two observations, we identified that solution alkalinity is critical for the effects of bamboo salt on membrane fluidity, as confirmed using three additional commercial bamboo salt preparations. Extended-DLVO model calculations support that the effects of bamboo salt on lipid membranes are due to the alkalinity imparting a stronger hydration force. Collectively, the results of this work demonstrate that processing of bamboo salt strongly affects its atomic composition and that the alkalinity of bamboo salt solutions contributes to its effect on membrane fluidity.

Keywords Cell membrane · Lipid bilayer · Mobility · Monovalent cation · Fluorescence recovery after photobleaching

J. H. Jeong, J.-H. Choi and M. C. Kim contributed equally to this work.

Electronic supplementary material The online version of this article (doi:10.1007/s00249-015-1043-8) contains supplementary material, which is available to authorized users.

✉ Nam-Joon Cho
njcho@ntu.edu.sg

1 School of Materials Science and Engineering, Nanyang Technological University, 50 Nanyang Avenue, Singapore 639798, Singapore

2 Centre for Biomimetic Sensor Science, Nanyang Technological University, 50 Nanyang Drive, Singapore 637553, Singapore

3 School of Chemical and Biomedical Engineering, Nanyang Technological University, 62 Nanyang Drive, Singapore 637459, Singapore

4 Department of Chemistry, College of Natural Science, Hanyang University, Seoul 133791, Korea

5 Department of Neurology, College of Medicine, Hanyang University, Seoul 133791, Korea

6 Department of Convergence Nanoscience, College of Natural Science, Hanyang University, Seoul 133070, Korea

Introduction

Bamboo salt has been used as a traditional Oriental medicine for over 1300 years and is widely used in household and food applications (Shin et al. 2003; Zhao et al. 2013a).

In recent years, in-depth studies have been launched focusing on characterizing the properties of bamboo salt and understanding its potential medical efficacy (Ha and Park 1998, 1999; Kim et al. 1998). Kim et al. reported the antiallergic effect of bamboo salt by demonstrating the inhibition of IgE antibody production and inflammatory cytokines (Kim et al. 2012). In a separate study, Shin et al. (2003, 2004) also showed the antiinflammatory activity of bamboo salt, and Zhao et al. (2013a, b) presented its anticancer activity. Numerous studies are ongoing to assess the validity of the claimed bamboo salt benefits and to understand the underlying mechanisms leading to the observed effects. Such studies aim to promote awareness of bamboo salt as a modern medicine and to delineate the molecular basis for its claimed health benefits.

The packaging of beneficial minerals in bamboo salt is because of its production procedure. Typically, sun-dried sea salt is first placed in a bamboo case, then sealed with yellow soil and baked at a temperature of over 1000 °C with fire fueled by pinewood and pine resin. Depending on the number of baking cycles, amalgamation of purified essential minerals from the bamboo trunk, yellow soil, pinewood and pine resin can be controlled (Shin et al. 2004a; Hu et al. 2000). Nine-times-baked bamboo salt (BS9x), also called purple bamboo salt because of its color, is claimed to have the most ideal amounts of minerals, including high concentrations of iron, silicon, and potassium, along with minimal impurities (Choi et al. 2012). BS9x also contains significant amounts of alkaline minerals such as calcium, magnesium, and sodium, rendering BS9x solutions alkaline (Ha and Park 1998; Shin et al. 2004b). It has been suggested that BS9x helps in the reinforcement of cellular protection capabilities, specifically through interactions with the lipid membrane to combat various diseases such as microbial, dental, inflammatory, and cardiovascular diseases, cancer, and diabetes (Shin et al. 2003, 2004b; Zhao et al. 2013a, b, c; Choi et al. 2012; Moon et al. 2009). However, cellular studies have remained inconclusive on the effect of bamboo salt on lipid membranes, largely because of the complexity of factors at play in biological systems.

Phospholipid assemblies on solid supports provide a reductionist approach to investigate the molecular mechanisms involving lipid membranes by using simplified models (Sackmann 1996; Czolkos et al. 2011). Specifically, lipid bilayers mimic the fundamental architecture of the cell membrane and can form two-dimensional planar bilayers or a layer of adsorbed lipid vesicles. In combination with a wide range of surface-sensitive measurement techniques, these platforms can be useful to study the structure and function of lipid bilayers under different environmental conditions and for applications such as molecular recognition and tracking enzymatic activity [see (Mashaghi et al. 2014) and references therein]. While many studies have been performed using different salt conditions (e.g., buffer, ionic strength) and delineated the corresponding effects on membrane formation and functionality (Böckmann et al. 2003; Jackman et al. 2013; Reimhult et al. 2003; Zimmermann et al. 2009), there have been no studies that investigate the influence of bamboo salt on artificial lipid membranes. Herein, we address this subject and focus on how bamboo salt affects the properties of supported lipid bilayers on glass substrates.

Materials and methods

Salt preparation

Dry samples of salts were prepared as follows: purified table salt (PS), sea salt (SS), one-time-baked bamboo salt (BS1x), three-times-baked bamboo salt (BS3x), five-times-baked bamboo salt (BS5x), and nine-times-baked bamboo salt (BS9x). Bamboo salt was produced by roasting sea salt from the Korean west coast in a bamboo trunk sealed with yellow clay over a furnace fueled by native Korean pinewood and pine resin. The bamboo was more than 3 years old and from the Damyang region in Korea, and the yellow clay was prepared from soil (natural illite clay) collected in the Gangwon Province mountains in Korea. The number of baking cycles, each consisting of 10 h of roasting (in excess of 900 °C), determined the resulting product. For solution experiments, the salts were dissolved in deionized water at a stock concentration of 3.75 M solution and diluted accordingly before the experiment. In addition, three commercial bamboo salt preparations were purchased from Kaeam Trading Co., Ltd., and tested. These commercial salts included twice-baked mineral bamboo salt (sample 1), mulberry bamboo salt (sample 2), and yellow ocher bamboo salt (sample 3). Aqueous salt solutions were prepared as described above.

Vesicle preparation

Extruded small unilamellar vesicles (SUVs) were prepared using 1-palmitoyl-2-oleoyl-*sn*-glycero-3-phophocholine (POPC) lipid (Avanti Polar Lipids, Alabaster, AL, USA). For fluorescence microcopy experiments, 0.5 mol % rhodamine-conjugated 1,2-dihexadecanoyl-*sn*-glycero-3-phophoethanolamine (Rhodamine-DHPE) (Avanti Polar Lipids) was added. Briefly, as-supplied lipids in chloroform were mixed to the desired molar amount in a glass tube, and then a dried lipid film was formed by drying with a gentle stream of nitrogen air followed by storage in a vacuum desiccator. The dried lipid film was then hydrated in 10 mM Tris buffer (pH 7.5) with 150 mM NaCl to a nominal concentration of 5 mg/ml. Lipid extrusion was performed using 27 cycles through a 50-nm

diameter track-etched polycarbonate membrane (Whatman Schleicher, Germany), followed by an additional 27 cycles through a 30-nm diameter membrane. The vesicle diameter and polydispersity of 64.5 ± 0.4 nm and 0.041 ± 0.008, respectively, were measured by dynamic light scattering measurements. Finally, vesicles were diluted in 10 mM Tris buffer to a fixed lipid concentration of 0.2 mg/ml prior to the experiment. All solutions were prepared with 18.2 MΩ cm Milli-Q water (Millipore, Billerica, MA).

Epifluorescence microscopy

Fluorescence microscopy imaging of supported lipid bilayers containing 0.5 wt% rhodamine-DHPE was performed by using an inverted epifluorescence Eclipse TE 2000 microscope (Nikon) equipped with a 60× oil immersion objective (NA 1.49) and an Andor iXon + EMCCD camera (Andor Technology, Belfast, Northern Ireland). The acquired images consisted of 512 × 512 pixels with a pixel size of 0.267 × 0.267 μm. The samples were illuminated through a TRITC (rhodamine–DHPE) filter set by a mercury lamp (Intensilight C-HGFIE; Nikon Corporation).

Fluorescence recovery after photobleaching (FRAP) analysis

For FRAP measurements, a 20-μm-wide circular spot was photobleached with a 532-nm, 100-mW laser beam, followed by time-lapsed recording. Diffusion coefficients were determined by the Hankel transform method (Jonsson et al. 2008) along with the immobile fraction. For all fluorescence imaging experiments, glass coverslips (Menzel Gläser, Braunschweig, Germany) were used together with commercially available microfluidic flow cells (stick-Slide I0.1 Luer, Ibidi, Munich, Germany), with an injection flow rate of 50 μl/min.

Laser ablation-inductively coupled plasma (LA-ICP) mass spectrometry

In situ quantitative trace element analyses were performed by LA-ICP-MS, which is a highly sensitive technology utilizing fine particles through laser ablation to chemically analyze the elements on a solid surface down to parts per billion (ppb level) without complicated sample preparation. The system consists of an Analyte G2 193-nm ArF excimer laser (Teledyne CETAC-Photon Machines) coupled to a iCAP Q mass spectrometer (Thermo Scientific). High-purity helium was used as a carrier gas. For rock salt samples (powder form), a 60-μm^2 spot was used to perform line scans of 300 μm length across the surface of multiple particles at a rate of 10 mm/s, a pulse rate of 10 Hz, and an energy fluence rate of 3.0 J/cm^2. For lipid samples, a 150 μm^2 spot was used to perform line scans of 1 mm in length at a rate of 33.10 mm/s, a pulse rate of 10 Hz, and an energy fluence of 1.4 J/cm^2. The isotopes ^{7}Li, ^{11}B, ^{23}Na, ^{25}Mg, ^{26}Mg, ^{27}Al, ^{29}Si, ^{31}P, ^{39}K, ^{42}Ca, ^{44}Ca, ^{49}Ti, ^{51}V, ^{53}Cr, ^{54}Fe, ^{55}Mn, ^{60}Ni, ^{63}Cu, ^{64}Zn, ^{65}Cu, ^{85}Rb, ^{86}Sr, ^{95}Mo, ^{98}Mo, and ^{133}Cs were monitored. NIST 610 glass reference standard was used for external calibration with the preferred values of Jochum et al. (2005).

Results and discussion

Characterization of bamboo salts

A wide variety of experimental conditions have been reported to influence the properties of supported lipid bilayers, including ionic strength, solution pH, and temperature. In order to examine the effects of bamboo salt on lipid bilayers, we first characterized a series of unprocessed and processed bamboo salt solutions. Indeed, there have been many reports on different variants of bamboo salt in the literature, and establishing fundamental knowledge about sample properties is important for comparison across different studies. We first measured the solution of bamboo salt, which is commonly referred to as an alkalizing agent (Zhao et al. 2012). For these experiments, dried salt samples were hydrated with deionized water to a final concentration of 1.7 M and then the solution pH was determined (Table 1). Unprocessed sea salt solution was prepared along with BS1x, BS3x, BS5x, and BS9x solutions. The unprocessed sea salt solution was mildly alkaline (pH ~8), while the processed bamboo salt solutions had more appreciable alkalinity (pH ~10.5), which is in line with previous reports (Zhao et al. 2012).

To further determine the chemical composition of the bamboo salt samples, laser ablation inductively coupled plasma mass spectrometry (LA-ICP-MS) experiments were conducted using dried samples in powder form. The salts mainly consisted of four major alkaline minerals, sodium, magnesium, potassium, and calcium, and the chloride salts

Table 1 Alkalinity of precursor and processed bamboo salt solutions

Salt (1.7 M)	pH
PS	7.00 ± 0.01
SS	7.88 ± 0.02
BS1x	10.26 ± 0.01
BS3x	10.21 ± 0.02
BS5x	10.43 ± 0.02
BS9x	10.61 ± 0.03

Standard conductivity measurements were performed in order to measure the pH value of bamboo salt solutions. The values are the average ± standard deviation of three measurements

Table 2 Elemental analysis of precursor and processed bamboo salt solutions

Isotope	SS	BS1x	BS9x
NaCl (%)	95.92	97.13	97.63
$MgCl_2$ (%)	3.54	1.86	0.17
KCl (%)	0.43	0.27	1.92
$CaCl_2$ (%)	0.11	0.75	0.27
P	n/d	17.78	1386.02
Fe	190	203.86	1830.35
Mn	11	36.40	124.24
Al	134.00	135.54	13.39
Si	565	853	274.02
Rb[a]	0.7	1.06	17.11
Sr[a]	44	156.62	109.37
Mo[a]	0.12	0.22	81.53
Cs[a]	0.03	0.03	0.15
V[a]	2.50	1.96	5.61

LA-ICP mass spectra were obtained for different bamboo salt solutions. Major elements are reported as weight percentage of chloride compounds

[a] Trace elements are reported in ppm

n/d not determined

of these four minerals are reported by w/w % percentage (Table 2). All other trace elements are reported in units of parts per million. Compared to the SS control, BS9x salt had slightly higher contents of sodium (97.63 vs. 95.92 %) and a fivefold increase in potassium (1.92 vs. 0.43 %). However, the magnesium content was reduced by 20-fold (0.17 vs. 3.54 %). The fractions of many trace elements increased significantly in the BS9x salt, including a 1000-fold increase in phosphorus, tenfold increase in iron, and tenfold increase in manganese. In addition, there was evidence of several minerals (e.g., rubidium, vanadium, etc.) that have not been previously identified in bamboo salt solutions, and at least some of these molecules are reported to have medical benefits (Petanidis et al. 2013; Brewer 1984; Peng et al. 2010; Reiss et al. 2005). In the context of lipid membrane properties, it is unlikely that these trace minerals exert an appreciable direct effect on the global properties of the lipid membrane. Rather, it appears that the alkalinity and/or presence of divalent cations (e.g., Mg, Ca) may influence the properties of lipid membranes, and we tested this hypothesis by performing FRAP experiments.

Influence of salt type on supported membrane fluidity

In order to investigate the effects of bamboo salt solution on lipid membrane properties, a fluorescently labeled supported lipid bilayer was formed on a glass substrate by the vesicle fusion method. Extruded POPC lipid vesicles containing 0.5 wt% rhodamine-POPC fluorescent lipids were prepared in 10 mM Tris buffer (pH 7.5) with 150 mM NaCl and deposited on the glass substrate. Under these conditions, the vesicles adsorb until reaching a critical surface coverage and then rupture to form a two-dimensional supported lipid bilayer (Keller and Kasemo 1998). Upon vesicle addition, a homogenous lipid bilayer was visualized by epifluorescence microscopy. FRAP analysis was performed by bleaching a 20-μm-wide circular spot of lipids in the bilayer, then measuring the return of fluorescence intensity to the spot as a function of time. Using the Hankel transform method, a diffusion coefficient of 2.4 ± 0.1 $\mu m^2/s$ was calculated for the control POPC lipid bilayer in 150 mM NaCl along with a mobile fraction of 90 ± 2 %. Then, a buffer exchange was performed in order to introduce 150 mM bamboo salt solution into the measurement chamber, followed by an equilibrium period. A FRAP measurement was next performed, and the time-lapsed snapshots are presented in Fig. 1. Quartz crystal microbalance with dissipation (QCM-D) measurements confirmed formation of supported lipid bilayers and demonstrated that the effects of ionic strength on the bilayer mass and viscoelastic properties are largely reversible (Figure S1). A series of buffer exchanges followed, with increasing concentrations of bamboo salt and FRAP measurements conducted at each condition.

Even at relatively low ionic strength, the bamboo salt solution had an appreciable effect on the diffusion coefficient, shifting the value to 3.2 ± 0.1 $\mu m^2/s$ at 150 mM bamboo salt solution. The increase in fluidity is likely due to more repulsive lipid-substrate interaction in the more alkaline condition of bamboo salt solution. At higher bamboo salt concentrations, the fluidity increased further. The diffusion coefficient was 3.6 ± 0.2 $\mu m^2/s$ at 1000 mM bamboo salt solution, then reached approximately 5.2 ± 0.5 $\mu m^2/s$ above 2000 mM bamboo salt solution and higher concentrations. With increasing salt concentration, the mobile fraction of lipids also increased to greater than 95 %. Importantly, the same trends in the diffusion coefficient and mobile fraction were reproduced using three commercial bamboo salt preparations (Figures S2–S4). Similar results were also obtained using Tris buffer solutions with alkaline conditions (pH 10.5) (see Figure S5).

To distinguish between the effects of solution pH and ionic strength, we also performed FRAP experiments on lipid bilayers in saline solutions at pH 7.5, as presented in Fig. 2. Interestingly, with increasing ionic strength in this case, we observed very different trends as compared with more alkaline conditions. The diffusion coefficient decreased as a function of ionic strength, reaching 1.7 ± 0.1 $\mu m^2/s$ under high ionic strength conditions (above 2000 mM NaCl). Furthermore, the mobile fraction of lipids decreased significantly from 90 ± 2 % at 150 mM to 70 ± 1 % at 3750 mM. A comparison of all FRAP measurement results is presented in Fig. 3. The

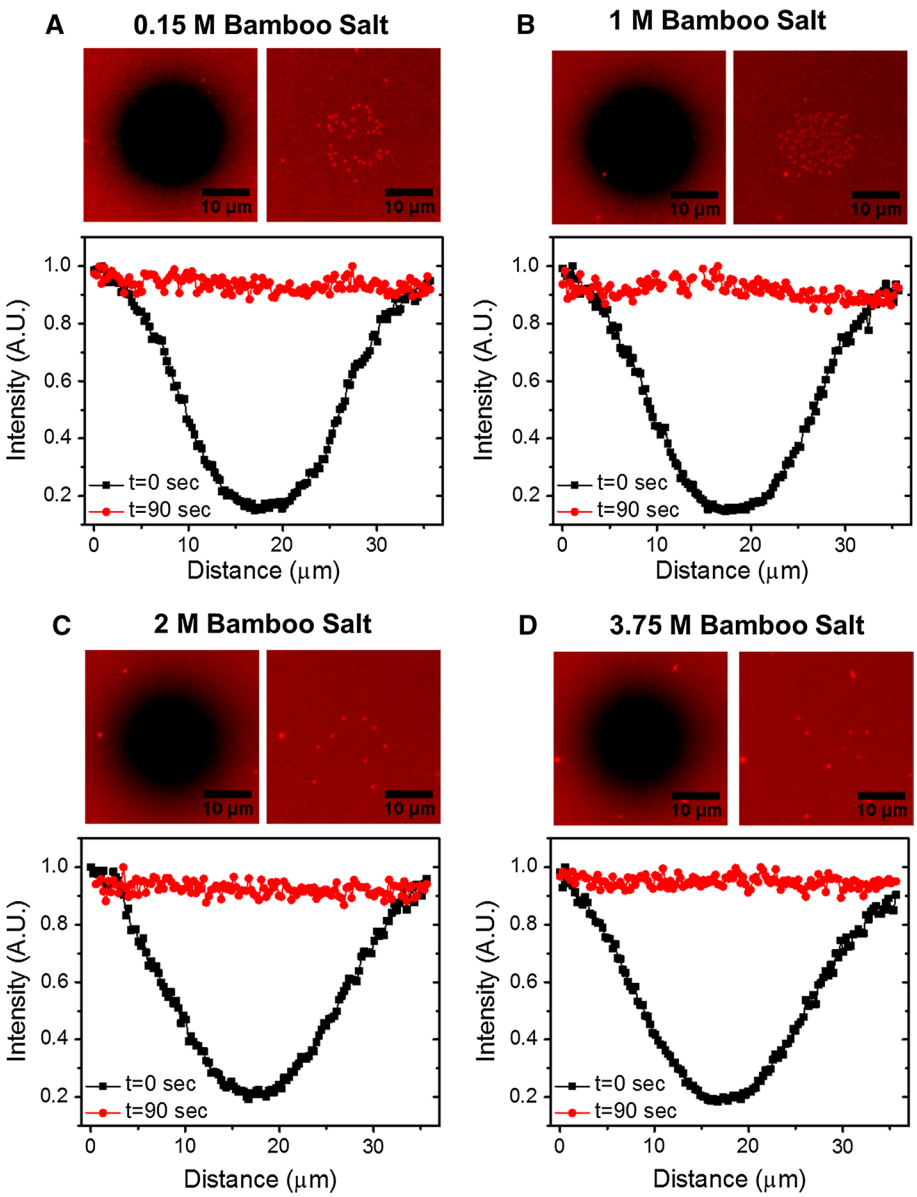

Fig. 1 Observation of alkaline bamboo salt effects on a supported lipid bilayer on glass. Epifluorescence microscopy was performed in order to visualize supported lipid bilayers in alkaline bamboo salt solutions. Panels **a**–**d** present time-lapsed fluorescence micrographs and intensity profiles of supported lipid bilayers incubated in bamboo salt solutions of varying ionic strength between 0.15 and 3.75 M. Photobleaching was performed at $t = 0$ min, and the bleached spot corresponds to the dark spot in the center of the micrograph. The *left* and *right* micrographs correspond to snapshots recorded at $t = 0$ and $t = 90$ s, respectively. The fluorescence intensity as a function of distance across the bleached spot at the two times is presented below the micrographs

observed trends are in good agreement with previous experiments reported by Böckmann et al. (2003). Hence, the effects of ionic strength depend on the solution pH, and it appears that the higher pH preserves the membrane fluidity. Specifically, under near-neutral pH conditions, higher ionic strength leads to a minor decrease in fluidity and significant drop in the mobile fraction, whereas, under alkaline conditions, higher ionic strength leads to a significant increase in fluidity and a very high mobile fraction.

Extended-DLVO model of lipid-substrate interactions

To understand the effects of different salts and corresponding solution conditions, we performed extended-DLVO model calculations (Jackman et al. 2013, 2014a; Nabika et al. 2008; Tero et al. 2008) that took into account the interfacial forces between the supported lipid bilayer and solid support and assumed monovalent salt conditions. Specifically, the model treats the bilayer and substrate as two parallel planes coming into contact and estimates the total interaction energy as a function of the separation distance between the bilayer and substrate. In an equilibrium configuration, the separation distance is predicted to be optimized so that it minimizes the interaction energies of the van der Waals force (always attractive), the double-layer electrostatic force (can be either repulsive or attractive; repulsive in our case based on the conditions and materials), and the hydration force (always repulsive; the magnitude is important). Accordingly, the total interaction

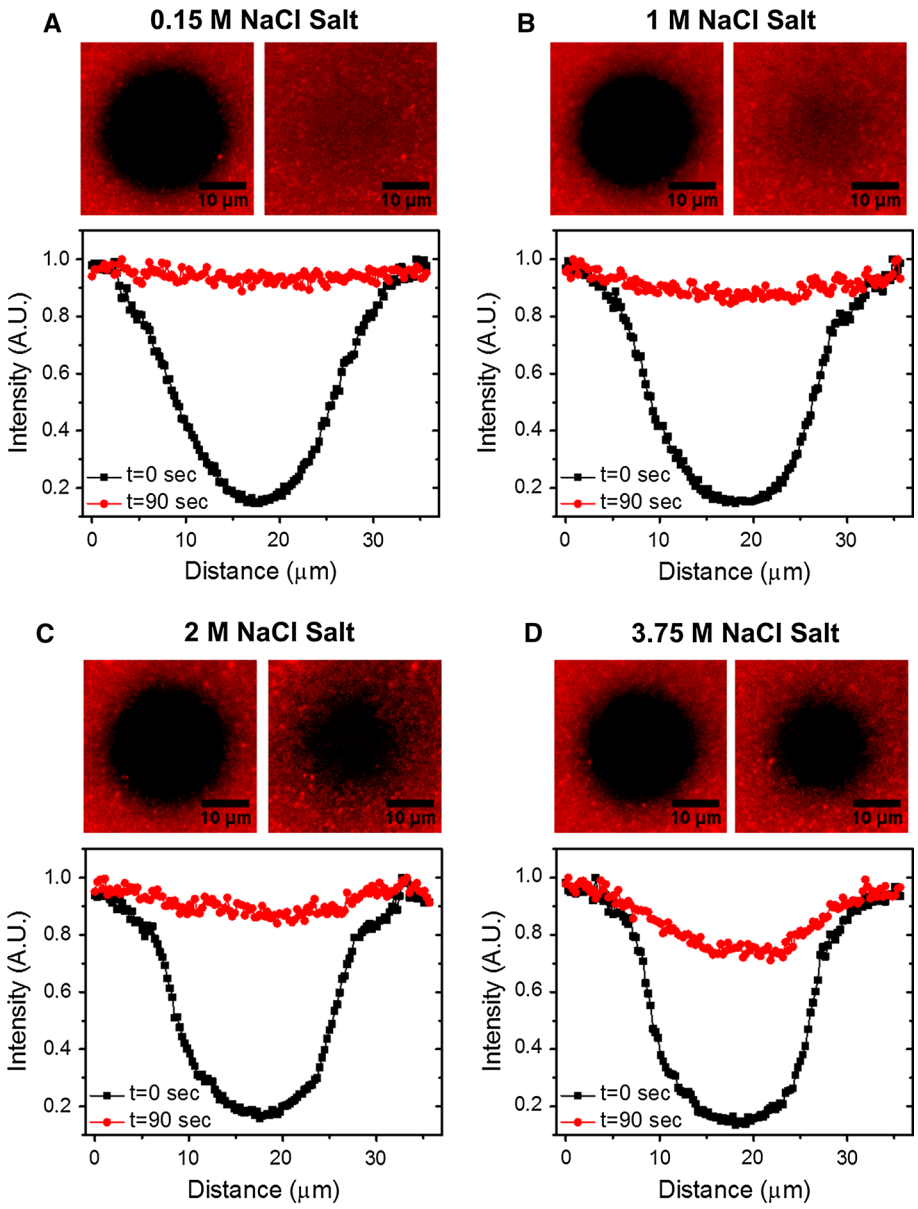

Fig. 2 Influence of ionic strength on the fluidity of a supported lipid bilayer on glass under near-neutral solution conditions. Similar epifluorescence microscopy experiments were conducted in order to visualize supported lipid bilayers in pH 7.5 Tris buffer solution with added sodium chloride. Panels **a**–**d** present time-lapsed fluorescence micrographs and intensity profiles of supported lipid bilayers incubated in pH 7.5 Tris buffer solutions of varying ionic strength

energy (W) as a function of separation distance (D) is represented by

$$W = W_{\mathrm{vdW}} + W_{\mathrm{DL}} + W_{\mathrm{hyd}} \tag{1}$$

where W_{vdW}, W_{DL}, and W_{hyd} correspond to the van der Waals, double-layer electrostatic, and hydration interaction energies, respectively. The individual interaction energies are defined by the following set of equations:

$$W_{\mathrm{vdW}} = -\frac{A_{132}}{12\pi D^2} \tag{2}$$

where A_{132} is the Hamaker constant that is defined by $A_{132} = A_{v=0}(2\kappa D)e^{-2\kappa D} + A_{v>0}$, with κ representing the inverse Debye length. The Prieve-Russell approach was followed in order to calculate the Hamaker constant, and

$$W_{DL} = 64000 N_A kTI \tanh\left(\frac{e\psi_s}{4kT}\right)\tanh\left(\frac{e\psi_b}{4kT}\right)\frac{\mathrm{e}^{-\kappa D}}{\kappa} \tag{3}$$

where N_A, k, T, I, e, Ψ, and κ represent the Avogadro constant, Boltzmann constant, temperature, ion strength, elementary charge, surface potential, and Debye length, respectively, and

$$W_{hyd} = \lambda P_0 e^{-\frac{D}{\lambda}} \tag{4}$$

where the values λ and P_0 depend on the experimental conditions, e.g., solution pH, ionic strength, and substrate type. P_0 was fixed as 1.15×10^8 N/m^3, and the decay length, λ, of the hydration force was varied.

Based on these equations, we performed a series of calculations to estimate how ionic strength influences the

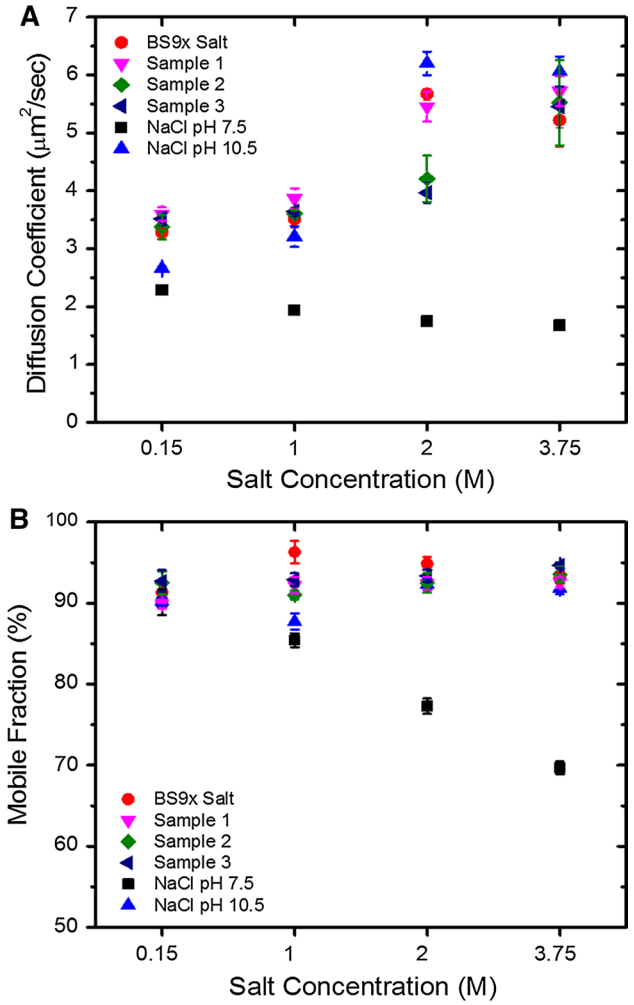

Fig. 3 FRAP analysis of supported lipid bilayers in the presence of different salts. Panels **a** and **b** present the experimentally measured diffusion coefficient and mobile fraction values, respectively, for supported lipid bilayers incubated in the presence of different salt solutions as a function of ionic strength. Each value is the average of three measurements, and the *error bar* represents the standard deviation

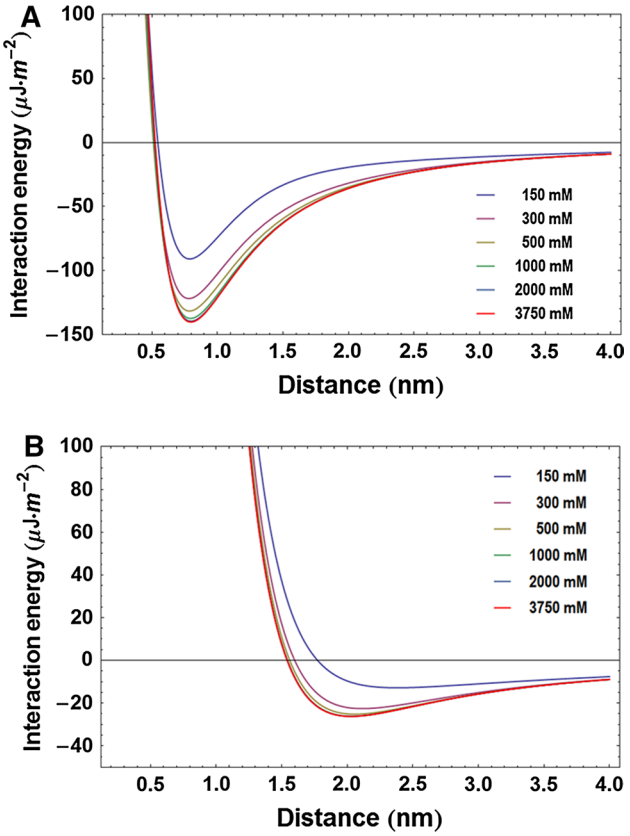

Fig. 4 Effects of ionic strength on the lipid-substrate interaction of a supported lipid bilayer. The lipid-substrate interaction between a supported lipid bilayer and silicon oxide was investigated as a function of separation distance by an extended-DLVO model. In the model calculations, the ionic strength condition was varied, with a fixed decay length of the hydration force. Panels **a** and **b** present the total interaction energy as a function of separation distance assuming either a weak (0.15-nm decay length) or strong (0.25-nm decay length) hydration force, respectively

lipid-substrate interaction. With increasing ionic strength, there was a minimal effect on the van der Waals force (Figure S6) and an appreciable effect on the double-layer electrostatic force (Figure S7). High salt concentrations lead to shielding, which retards the electrostatic force. In addition to these two forces, Jackman et al. (2014b) recently showed that the magnitude of the hydration force is a particularly sensitive indicator of the lipid-substrate interaction on titanium oxide. Cremer and Boxer (1999) have also previously reported that ice-like hydration layers form on silicon oxide under alkaline conditions and impede vesicle adhesion. Considering these points, we performed the model calculations by choosing two different magnitudes of the hydration force via changing the decay length of the force. The reported range (Kanduč et al. 2014) is between 0.1 and 0.6 nm, and we chose two values, 0.15 and 0.25 nm, which correspond to a relatively weak and strong hydration force, respectively, for a lipid bilayer on silicon oxide (see Figure S8).

Under a relatively weak hydration force (i.e., the near-neutral pH case), we observed that the lipid-substrate interaction was always attractive and had an equilibrium separation distance predicted to be around 0.7 nm (Fig. 4a). Interestingly, the ionic strength had an appreciable effect on the estimated total interaction energy of the system at the equilibrium position. At 150 mM salt, the total interaction energy was -70 μJ/m^2. With increasing salt concentration, the total interaction significantly decreased to -130 μJ/m^2 at 300 mM salt followed by reaching a maximum saturation value around -140 μJ/m^2 for higher salt concentrations. Importantly, Mager et al. (2008) have established a relationship between the bilayer-substrate separation distance

(in turn reflecting the lipid-substrate interaction) and membrane fluidity, and our FRAP and extended-DLVO model calculations are consistent with the proposed relationship. In particular, we observe that membrane fluidity decreases with increasing ionic strength, and this finding is consistent with the prediction that the lipid-substrate interaction becomes stronger with increasing ionic strength. Hence, due to the stronger lipid-substrate interaction, the diffusion coefficient decreases along with an increase in the immobile fraction.

On the contrary, under a relatively strong hydration force (i.e., the alkaline case), we observed that the lipid-substrate interaction was attractive, albeit much weaker, and the energy minimum was very shallow (Fig. 4b). For 150 mM salt, the total interaction energy was -15 μJ/m^2 at the equilibrium position. With increasing salt concentration, the total interaction energy reached -22 μJ/m^2 at 300 mM salt and above. Interestingly, in the FRAP experiments, we observed that the membrane fluidity continued to increase as a function of ionic strength in this salt concentration regime for bamboo salt solutions. Together with the model calculations, this evidence supports that the increase in membrane fluidity under alkaline conditions is due to both lipid-substrate and lipid-salt interactions. Hence, the data suggest that bamboo salt increases the fluidity of lipid membranes by imparting an alkaline environment along with additional effects, the specifics of which remain to be further investigated in future work. Considering that many types of bamboo salt are known to promote alkalizing environments (Ha and Park 1998; Shin et al. 2004b), we anticipate these other salts would have similar effects on lipid membranes. From a human health perspective, it is well established that the body operates well in a slightly alkaline environment. Bamboo salts help to ensure this condition, and it will be important to understand the interplay of membrane fluidity and alkaline conditions in the context of optimal cellular function.

Conclusion

In this work, we have investigated the effect of bamboo salt on lipid membranes by employing supported lipid bilayers. Compared to previous bamboo salt studies, this work is, to the best of our knowledge, the first that employs a reductionist approach using a simplified model membrane system that permits characterization by surface-sensitive characterization tools, e.g., the FRAP and QCM-D measurement techniques. Using this approach, we identified that alkaline bamboo salt solutions, including commercial samples, increase membrane fluidity with increasing ionic strength. Similar observations were made using alkaline buffer solutions with saline solutions. By contrast, near-neutral saline solutions yielded less-fluid bilayers, and high ionic strengths in this case retarded membrane fluidity. Our theoretical extension of this work with extended-DLVO model calculations support that the hydration force plays an important role in influencing bilayer fluidity. Based on the findings of this work, including the identification of novel elements in bamboo salt and observed influence of alkalinity on membrane fluidity, one can envision several interesting lines of future research related to the investigation of bamboo salt with supported lipid membranes.

References

Böckmann RA, Hac A, Heimburg T, Grubmüller H (2003) Effect of sodium chloride on a lipid bilayer. Biophys J 85:1647–1655

Brewer AK (1984) The high pH therapy for cancer tests on mice and humans. Pharmacol Biochem Behav 21(Suppl 1):1–5

Choi CH, Ha MO, Youn HJ, Jeong SS, Iijima Y et al (2012) Effect of bamboo salt-NaF dentifrice on enamel remineralization. Am J Dent 25:9–12

Cremer PS, Boxer SG (1999) Formation and spreading of lipid bilayers on planar glass supports. J Phys Chem B 103:2554–2559

Czolkos I, Jesorka A, Orwar O (2011) Molecular phospholipid films on solid supports. Soft Matter 7:4562–4576

Ha JO, Park KY (1998) Comparison of mineral contents and external structure of various salts. J Korean Soc Food Sci Nutr 27:413–418

Ha JO, Park KY (1999) Comparison of autooxidation rate and comutagenic effect of different kinds of salt. J Korean Assoc Cancer Prev 4:44–51

Hu C, Zhang Y, Kitts DD (2000) Evaluation of antioxidant and prooxidant activities of bamboo *Phyllostachys nigra* var. Henonis leaf extract in vitro. J Agric Food Chem 48:3170–3176

Jackman JA, Choi J-H, Zhdanov VP, Cho N-J (2013) Influence of osmotic pressure on adhesion of lipid vesicles to solid supports. Langmuir 29:11375–11384

Jackman JA, Zhao Z, Zhdanov VP, Frank CW, Cho N-J (2014a) Vesicle adhesion and rupture on silicon oxide: influence of freeze-thaw pretreatment. Langmuir 30:2152–2160

Jackman JA, Goh HZ, Zhao Z, Cho N-J (2014b) Contribution of the Hydration Force to Vesicle Adhesion on Titanium Oxide. Langmuir 30(19):5368–5372. doi:10.1021/la404581d

Jochum KP, Nohl L, Herwig K, Lammel E, Toll B et al (2005) GeoReM: a new geochemical database for reference materials and isotopic standards. Geostand Geoanal Res 29:333–338

Jonsson P, Jonsson MP, Tegenfeldt JO, Höök F (2008) A method improving the accuracy of fluorescence recovery after photobleaching analysis. Biophys J 95:5334–5348

Kanduč M, Schlaich A, Schneck E, Netz RR (2014) Hydration repulsion between membranes and polar surfaces: simulation approaches versus continuum theories. Adv Colloid Interface Sci 208:142–152

Keller C, Kasemo B (1998) Surface specific kinetics of lipid vesicle adsorption measured with a quartz crystal microbalance. Biophys J 75:1397–1402

Kim SH, Kang SY, Jung KK, Kim TG, Han H-M et al (1998) Characterization and anti-gastric ulcer activity of bamboo salt. J Food Hyg Safe 13:252–257

Kim KY, Nam SY, Shin TY, Park KY, Jeong HJ et al (2012) Bamboo salt reduces allergic responses by modulating the caspase-1 activation in an OVA-induced allergic rhinitis mouse model. Food Chem Toxicol 50:3480–3488

Mager MD, Almquist B, Melosh NA (2008) Formation and characterization of fluid lipid bilayers on alumina. Langmuir 24:12734–12737

Mashaghi A, Mashaghi S, Reviakine I, Heeren RM, Sandoghdar V et al (2014) Label-free characterization of biomembranes: from structure to dynamics. Chem Soc Rev 43:887–900

Moon JH, Shin HA, Rha YA, Om AS (2009) The intrinsic antimicrobial activity of bamboo salt against salmonella enteritidis. Mol Cell Toxicol 5:323–327

Nabika H, Fukasawa A, Murakoshi K (2008) Tuning the dynamics and molecular distribution of the self-spreading lipid bilayer. Phys Chem Chem Phys 10:2243–2248

Peng SL, Liu XS, Wang T, Li ZY, Zhou GQ et al (2010) In vivo anabolic effect of strontium on trabecular bone was associated with increased osteoblastogenesis of bone marrow stromal cells. J Orthop Res 28:1208–1214

Petanidis S, Kioseoglou E, Hadzopoulou-Cladaras M, Salifoglou A (2013) Novel ternary vanadium-betaine-peroxido species suppresses H-ras and matrix metalloproteinase-2 expression by increasing reactive oxygen species-mediated apoptosis in cancer cells. Cancer Lett 335:387–396

Reimhult E, Höök F, Kasemo B (2003) Intact vesicle adsorption and supported biomembrane formation from vesicles in solution: influence of surface chemistry, vesicle size, temperature, and osmotic pressure. Langmuir 19:1681–1691

Reiss J, Bonin M, Schwegler H, Sass JO, Garattini E et al (2005) The pathogenesis of molybdenum cofactor deficiency, its delay by maternal clearance, and its expression pattern in microarray analysis. Mol Genet Metab 85:12–20

Sackmann E (1996) Supported membranes: scientific and practical applications. Science 271:43–48

Shin HY, Lee EH, Kim CY, Shin TY, Kim SD et al (2003) Anti-inflammatory activity of Korean folk medicine purple bamboo salt. Immunopharmacol Immunotoxicol 25:377–384

Shin HY, Na HJ, Moon PD, Seo SW, Shin TY et al (2004a) Biological activity of bamboo salt. Food Ind Nutr 9:36–45

Shin HY, Na HJ, Moon PD, Shin T, Shin TY et al (2004b) Inhibition of mast cell-dependent immediate-type hypersensitivity reactions by purple bamboo salt. J Ethnopharmacol 91:153–157

Tero R, Ujihara T, Urisu T (2008) Lipid bilayer membrane with atomic step structure: supported bilayer on a step-and-terrace TiO2 (100) surface. Langmuir 24:11567–11576

Zhao X, Jung OS, Park KY (2012) Alkaline and antioxidant effects of bamboo salt. J Korean Soc Food Sci Nutr 41:1301–1304

Zhao X, Kim SY, Park KY (2013a) Bamboo salt has in vitro anticancer activity in HCT-116 cells and exerts anti-metastatic effects in vivo. J Med Food 16:9–19

Zhao X, Ju J, Kim HM, Park KY (2013b) Antimutagenic activity and in vitro anticancer effects of bamboo salt on HepG2 human hepatoma cells. J Environ Pathol Toxicol Oncol 32:9–20

Zhao X, Deng X, Park KY, Qiu L, Pang L (2013c) Purple bamboo salt has anticancer activity in TCA8113 cells in vitro and preventive effects on buccal mucosa cancer in mice in vivo. Exp Ther Med 5:549–554

Zimmermann R, Küttner D, Renner L, Kaufmann M, Zitzmann J et al (2009) Charging and structure of zwitterionic supported bilayer lipid membranes studied by streaming current measurements, fluorescence microscopy, and attenuated total reflection Fourier transform infrared spectroscopy. Biointerphases 4:1–6